

Laser Ablation Microthruster Technology*

John K. Ziemer[†]
Jet Propulsion Laboratory, M/S 125-109
California Institute of Technology
4800 Oak Grove Drive, Pasadena, CA 91109
(818) 393-4582, John.K.Ziemer@jpl.nasa.gov

AIAA-2002-2153[‡]

Abstract

A review of Laser Ablation Microthruster (LA μ T) technology along with recent experimental results are presented. The performance, system mass, and total impulse of various LA μ T concepts are compared to other pulsed microthruster technologies including the Micro-Pulsed Plasma Thruster (μ PPT) and Vacuum Arc Thruster (VAT). The LA μ T concepts are shown to be favorable for missions with sub-micronewton thrust or sub-micronewton-second impulse bit requirements. The LA μ T may also possess unique capabilities for distributed or remote propulsion requirements. To investigate potential thruster performance, lifetime, and propellant feed mechanism issues, a laser ablation experiment has been setup at JPL. Using a diode-pumped, passively Q-switched Nd:YAG microlaser operating at 532 nm, ablation of aluminum has been studied in an ultra-high vacuum (UHV) chamber with a time-of-flight Faraday probe. Experimental results show that increasing background pressure from 10^{-7} to 10^{-4} Torr changes the measured peak ion velocity and current density in single pulse experiments. In measurements using the same site for multiple (≤ 2000) ablation pulses, peak ion velocity and current density decrease with increasing pulse number due to the deposition of target material towards the laser source. Pulse and burst frequency also influence current decay rates. In some cases, the peak current density recovers to nearly 75% of its original value following a pause between pulses or bursts > 10 s.

*Copyright ©2002 by the American Institute of Aeronautics and Astronautics, Inc. The U.S. Government has a royalty-free license to exercise all rights under the copyright claimed herein for Governmental purposes. All other rights are reserved by the copyright owner.

[†]Staff Engineer, Advanced Propulsion Technology Group. Member AIAA.

[‡]Presented at the 33rd AIAA Plasmadynamics and Lasers Conference, Maui, HI, May 2002.

1 Introduction

Micropropulsion devices that are designed to produce micronewton level thrust or micronewton-second level impulses are being developed in many industrial, government, and academic laboratories around the world [1]. This effort is in response to missions that plan to use microspacecraft or require extremely precise thrust levels. For example, many upcoming missions such as TechSat21, LISA, ST7, STEP, MICROSCOPE, EX5, LIRE, MAXIM, TPF, and Stellar Imager will require various microthrusters that can provide between 1-1000 μ N with precision requirements as small as 0.1 μ N and minimum impulse bits as small as 1 μ Ns.

The Laser Ablation Microthruster (LA μ T)¹ is one propulsion device that could meet these precision thrust requirements. As a microthruster concept, a LA μ T produces micronewton level thrust by using a low power (< 10 W) laser to ablate a variety of different propellant materials including metals and polymers. Typically diode or diode-pumped lasers are used for their compact size and relatively efficient operation. Recently, LA μ Ts have experienced a surge of research activity as all-solid-state lasers with enough intensity for ablation are becoming commercially available in small packages [2–9]. Although laser ablation can be used effectively for much larger thrust applications as well [10], this paper will focus on the micropropulsion applications.

We begin with a review of the most recent concepts for LA μ Ts and the basic physical principles behind their operation. We will also discuss the various laser technologies used in these thruster designs. Next, we compare this technology in terms of system-level criteria with other pulsed microthrusters that operate in nearly the same regime of impulse and thrust. To investigate the perfor-

¹This acronym is introduced here in a generic sense and is meant to apply to any of the various micro-sized thrusters that use laser ablation as the primary acceleration mechanism

mance of these microthrusters, a laser ablation experiment has been setup recently at JPL and will be described here in detail. Preliminary results including the effects of background pressure, pulse rate, and burst duty cycle will be presented and discussed in terms of implications for future performance measurements.

2 Microthruster Technology

Microthruster technology is a key element for enabling small-, micro-, and nano-satellites as well as a large class of missions that operate in a “drag free” mode where propulsion requirements are on the micro-scale. A thorough review of microthruster technology including steady-state and impulsive thruster technologies can be found in Ref. [1]. Although over thirty different types of steady-state microthrusters (FEED, Colloid, Micro-Cold-Gas Thrusters, PPTs, etc.) are being evaluated for these class of missions, pulsed microthrusters have the unique capability to provide both small individual impulse bits and a relatively continuous thrust at higher pulse frequencies. To limit our review to a reasonable size, we will compare only *pulsed* microthruster technologies including relatively new developments in Laser Ablation Microthrusters (LA μ T). Although the power supplied to these device may be nearly steady-state in nature, in general, the output can be modulated to provide single or multiple pulses in bursts, which allows LA μ Ts to fall within this category.

In this section of the paper we will describe the performance criteria that will subsequently be used to compare various pulsed microthruster concepts. A description each of the systems: LA μ Ts, micro Pulse Plasma Thruster (μ PPT), and Vacuum Arc Thruster (VAT) will be followed by a discussion of how each concept responds to the performance criteria. It should be noted that all the concepts presented here are still under rapid development and thruster characteristics are expected to change quickly with time. The author’s intent here is to provide an unbiased examination of the various pulsed microthruster technologies at their current state of evolution while keeping future improvements in mind. Therefore, performance will only be quoted in general terms without referring to specific prototypes or design points except where specific data are available. Although the evaluation of each criteria may change as each technology develops, the performance criteria themselves should be more concrete.

2.1 Performance Criteria for Pulsed Microthrusters

Pulsed microthrusters are generally designed to produce the greatest amount of impulse for a given amount of input energy and propellant mass while using the smallest and most light-weight system possible. Although determining the most important criteria (impulse bit, efficiency, specific impulse, dry mass etc.) depends on the application, each technology can be evaluated based on quantitative measurements of various performance variables.

The performance criteria used for this study, in no particular order, are:

- Minimum impulse provided by a single pulse
- Energy consumed per pulse (supplied by spacecraft bus)
- Impulse bit repeatability
- Maximum thrust level (maximum pulse frequency²)
- Propellant mass utilization
- Power conditioning (or laser) efficiency
- Total impulse capability (and corresponding propellant mass)
- Total system mass
- Impact on spacecraft (contamination, EMI, etc.)
- Lifetime and reliability

Note that ratios of individual criteria (specific impulse, efficiency, etc.) can also be useful performance indicators although they are not included in this list directly. In our study, the normal ratios used for conventional primary propulsion systems may not be the most useful for microthruster technologies. For example, the conventional definition of specific impulse is the ratio of the total impulse provided by a certain mass of propellant to the weight of that propellant on the surface of the earth. This is a useful performance indicator for conventional rockets where the total mass is primarily propellant, and the spacecraft’s mass changes significantly over the course of a mission. In the case of microthruster technologies and secondary propulsion systems in general, often the propellant is not the largest fraction of the total propulsion system mass, and the spacecraft mass stays relatively fixed over the mission. Since total component mass is

²We assume the pulse frequency can be continually set between single pulse operation and the maximum pulse frequency of the device.

frequently more important for micro-spacecraft design, a better performance ratio would be the total impulse, I_{tot} divided by the total mass of the propulsion system, M_{tot} ,

$$\begin{aligned} I_{sptot} &\equiv \frac{I_{tot}}{M_{tot}} = \frac{M_{prop}u_e}{M_{dry} + M_{prop}} \\ &= \frac{I_{sp}g_0}{\frac{M_{dry}}{M_{prop}} + 1}. \end{aligned} \quad (1)$$

If the stored propellant mass, M_{prop} , dominates the total system mass (or equivalently the dry mass, M_{dry} , is relatively small), this relation would reduce to the exhaust velocity, u_e , or the conventional definition of specific impulse, I_{sp} .

Another important performance indicator is the ratio of the impulse bit, I_{bit} , to the energy *supplied by the spacecraft bus*, E_{sb} , for each pulse. Using the pulse frequency, f_p , this ratio is equivalent to the more familiar thrust-to-power ratio,

$$\frac{I_{bit}}{E_{sb}} = \frac{T}{P}. \quad (2)$$

In published pulsed thruster research, the energy per pulse is usually given in terms of the stored energy, E , or the laser output energy (fluence) and does *not* include any energy used for power conditioning or cooling, if necessary. The relation between the two energy values is simply

$$E = E_{sb}\eta_{pc}, \quad (3)$$

where η_{pc} is the power conditioning or laser efficiency including any power required for active cooling. In laser ablation literature the impulse-to-energy ratio (I_{bit}/E) is referred to as the momentum coupling constant, C_m . We can now define a propulsion system efficiency, η_{sys} ,

$$\begin{aligned} \eta_{sys} &\equiv \frac{I_{sptot}}{2} \frac{I_{bit}}{E_{sb}} = \frac{I_{sptot}}{2} \frac{I_{bit}}{E} \eta_{pc} \\ &= \frac{I_{sptot}}{2} C_m \eta_{pc}. \end{aligned} \quad (4)$$

The factor of two is included so that if, again, the propulsion system is dominated by propellant mass, the propulsion system efficiency is equivalent to the conventional definition of thrust efficiency and cannot be greater than unity.

Equations 1, 2, and 4 include many of the performance criteria listed above, and we will now discuss the remaining items. The minimum impulse bit and the repeatability of the nominal I_{bit} are also critical mission design parameters. Although they can be measured quantitatively, the measurement technique can be difficult to implement at these low-levels of impulse. Maximum thrust (or pulse

frequency) is often determined by the maximum available power on the spacecraft, but may be determined by other system limits such as capacitor charging time or diode temperature.

Other items such as the propellant utilization efficiency, spacecraft interactions, lifetime and reliability are system specific. The propellant utilization, η_{pu} , can be evaluated over the lifetime of the thruster and is defined as,

$$\eta_{pu} \equiv \frac{m_{bit} N_{ptot}}{M_{prop}}, \quad (5)$$

where m_{bit} is the mass ablated per pulse and N_{ptot} is the total number of pulses over the lifetime of the thruster. The lifetime of a pulsed thruster is often put in terms of a total number of pulses since capacitors, electrodes, or other electronics will often provide only a finite number of cycles before they can be expected to fail. Besides expected lifetime, non-predictable failures such as electrode shorting or propellant feed failure can also influence a more qualitative evaluation of reliability. Finally, spacecraft interactions such as EMI or contamination are important to consider for pulsed thrusters, especially those with short ($\leq 1\mu s$) discharges that use solid propellants. Still, frequently these potential problems can usually be mitigated by power supply design or thruster placement as long as the issues are quantified before the spacecraft design is finalized. Furthermore, since all the microthruster systems being compared here share the characteristic of using a solid propellant, concerns of spacecraft contamination will be universal until properly addressed for the specific mission.

Now that the criteria have been explained, we will examine each pulsed microthruster concept in detail.

2.2 Laser Ablation Microthruster Concepts

Compared to previous ground-based laser ablation concepts, the LA μ Ts are unique in that the laser is an integral part of the microthruster. Recent advances in solid state laser technology have allowed high brightness (≥ 1 W), high efficiency ($\sim 50\%$) diode lasers to be packaged in small, light-weight containers. These diode lasers can be used alone to produce ablation or as a pumping source for other types of solid-state lasers. Minimum impulse bits produced by laser ablation are likely to be the lowest of all pulsed microthrusters, providing either precise fine-pointing or low-noise thrust capability. Furthermore, the ablation and subsequent acceleration mechanism can be quite efficient compared to other low-power devices.

The general operation principle for LA μ Ts relies on a tightly focused, high intensity laser source to deposit a relatively large amount of energy to a small area in a

short amount of time. As long as the target material does not have a high enough thermal conductivity to transport the energy away quickly, the local binding energy of the material can be exceeded, and a plasma will be produced near the surface [11]. Typically this plasma goes on to absorb or scatter a significant fraction of the remaining incoming light making the process somewhat self-limiting. The optimal condition occurs when the fluence threshold of ablation is just exceeded. The two important variables are then the fluence the laser provides during a pulse, Φ , (J/cm^2) and the time length of the pulse, τ . Phipps et al have developed an empirical relation based on over 40 independent measurements for determining the threshold fluence of ablation over a wide range of pulse durations, laser wavelengths, and materials [11]. Within a factor of three in most cases, the threshold relation is,

$$\Phi_{th} = (2.36 \times 10^4)(\tau)^{0.45}. \quad (6)$$

This can be an effective tool for determining if a particular laser technology can provide enough fluence for ablation to occur. Again, the likelihood of ablation can also be increased by choosing a propellant with a poor thermal conductivity.

Phipps [12] and others (see Refs. [13, 14], for example) have also developed relations for the impulse generated given an absorbed intensity, I_{ab} , laser wavelength, λ , pulse duration, and ionization state of the resulting plasma. In general, the relations reduce to the laser momentum coupling constant, C_m) that has the following proportionality,

$$C_m \propto (I_{ab}\lambda\sqrt{\tau})^k, \quad (7)$$

where k is a constant ≈ -0.3 . This relation allows us to estimate the impulses produced by a Laser Ablation Microthruster for a given laser technology. In general, values of C_m can be quite large compared to values of I_{bit}/E for other acceleration mechanisms. As observed by multiple investigators, the efficiency of the laser ablation process can be higher than 60% with ion velocities higher than 20 km/s [10, 15, 16]. Peaked velocity distributions have also been observed showing higher power ($n > 1$) cosine (\cos^n) distributions [17]. It has also been shown that the expanding plasma can form into a thin shell at higher background pressure yielding a narrow velocity distribution [18].

Recently all-solid-state, low-power lasers have become bright enough to produce ablation. Specifically diode lasers and diode-pumped lasers have been used to explore two different LA μ T concepts. We will now describe each program in more detail.

2.2.1 Diode Laser Driven Microthruster

Claude Phipps along with researchers at the University of New Mexico have designed, built, and tested a microthruster driven by a steady-state diode laser [2–4]. Using a transparent tape coated with PVC material on one side, a 1 W 935 nm diode laser is used to ablate the propellant either transmitting through the tape (which protects the optics but provides a lower performance) or reflecting off the front surface. Although the diode laser alone is quite efficient, and it can be pulsed creating fairly high fluence, the ablation threshold is not reached for metals, limiting propellant choice to various polymers.

Both single pulse and steady-state measurements of impulse and thrust have been conducted on a thrust stand. Typical measured values of the momentum coupling constant are close to 100 μ N/W with specific impulse values between 100-1000 s. For the thruster prototype, a low-mass tape feeding system has been developed and tested on a thrust stand, but issues of thrust vector control and system reliability are continuing to be addressed [2, 3].

2.2.2 Microchip Laser Thruster

David Gonzales and others at MIT Lincoln Laboratory have been using a 1 W diode laser as a pumping source for a Nd:YAG microchip crystal [7, 8] operating at 1064 nm. The entire cavity, including a passive Q-switch, can be contained in a volume so small that it can fit on the end of a standard fiber optic cable [19]. Although the overall efficiency of these lasers is much less than their diode pump counterpart (only 10% of the pump power is transmitted), the passive Q-switch creates short pulses on the order of nanoseconds with high instantaneous power, $> kW$. Instantaneous fluence levels are also higher, beyond the threshold for most materials including aluminum, copper, stainless steel, indium, and titanium, which were all tested in bench-top experiments at atmospheric pressure. Ablation crater profiles have been measured, and an piezoelectric disc bender has been used to measure impulses. Performance between 0.3 nN and 3 μ N has been inferred from measurements using a 100 mW output power (approximately 6.5 W input power) PowerChip Nanolaser. This gives a coupling constant of approximately 10 μ Ns/J and a thrust-to-power ratio of 0.2 μ N/W.

Although the efficiency of these devices reduces the overall performance significantly, this technology may be useful in other applications. For example, one diode laser could supply multiple microchip lasers distributed over the spacecraft. In addition, spacecraft structure or materials that are not needed after launch (aluminum, metalized kapton, etc.) could be used as propellant with the proper steering optics. Finally, in single shot operation,

this device could provide the lowest minimum impulse bit (< 1 nNs) of any propulsion system studied to date. Work is continuing on designing a microthruster prototype using this laser technology.

2.3 Micro-Pulsed Plasma Thruster

The Micro-Pulsed Plasma Thruster (μ PPT) is being developed by the Air Force for a technology demonstration mission on TechSat21 [20–22]. The μ PPT uses a high-voltage, capacitively driven arc discharge to ablate and accelerate insulation and electrode material (typically Teflon and copper, respectively) in a small diameter (≤ 0.25 in.) coaxial geometry. The acceleration process is a combination of plasma heating and expansion as well as a Lorentz force that helps to further expand the plasma front. The μ PPT can operate in a steady self-triggering mode or in a controlled pulsed mode, both of which require high voltage, > 1 kV, to initiate the discharge. However, the complexity of the self-triggering μ PPT driving electronics has been significantly reduced compared to conventional PPTs, reducing the dry mass by as much as 60X. Typical discharge energy is between 1–5 J producing an estimated 10 μ Ns of impulse. Preliminary thrust stand tests have been conducted to confirm these estimations with measured thrust-to-power ratios close to 5 μ N/W. Successfully completed long duration tests (> 1 million pulses) have begun to demonstrate the total impulse capability of this technology and provide engineers with important design information for future iterations.

The repeatability of the impulse bit depends to a large extent on the actual pulse energy and the initial placement of the arc within the electrode geometry. Modifications to electrode geometry and circuit design that are meant to improve the repeatability are being investigated. One potential lifetime limiting factor for this device is the possibility of some semi-ablated material condensing between the electrode surfaces. This could reduce the breakdown or hold-off voltage which would decrease the energy in each pulse, or provide a low resistance path for the power supply. Currently trade-offs between propellant area, electrode material, discharge energy, and discharge voltage are being evaluated to improve the μ PPT performance. Overall, by our evaluation, the system efficiency is close to 1%, mainly due to the relatively large dry mass and low total impulse capability. Again, design changes to improve total propellant throughput are ongoing.

2.4 Vacuum Arc Thruster

A vacuum arc thruster uses solid metal propellant that also serves as a cathode for an inductively driven arc discharge [23, 24]. To provide enough electrons to main-

tain the discharge, local cathode spot temperatures reach high enough values to ablate and produce a metal-vapor plasma. Depending on the metal, ion velocity from the surface can be as high as 30 km/s, although not all the propellant actually gets accelerated to the maximum ion speed. Still, thrust-to-power ratios have been measured on a thrust stand as high as 12 μ N/W with tungsten propellant, and other propellants may achieve as high as 20 μ N/W based on models of the discharge and measured physical properties of various materials. The relatively high thrust-to-power ratio is the result of an efficient, low-voltage, inductive energy storage unit providing the discharge current. This PPU can have a mass as small as 100 g leading to larger values of I_{spot} . The power and pulse rate can be set as high as 100 W and 200 Hz, respectively, leading to a large dynamic range of performance for this technology.

The largest concern for VAT technology is the perspective lifetime and propellant processing capability. Especially at higher powers, there is a chance of an electrical short occurring between the electrodes during operation. Although feedback circuitry has been added to increase reliability, a long duration test where performance is measured as a function of pulse number has not been conducted to date. Also, due to the ablative nature of the thruster and the driving circuit requirements, it may be difficult to feed metal propellant from behind the thruster. Currently other geometries and propellant holding mechanisms are being examined, along with the possibility of using many fixed thruster heads with one PPU. In addition, engineers at Alameda Applied Sciences Corp. are planning to launch a VAT on a University of Illinois Cube Sat. Again, the major advantage with this technology that leads to a high system efficiency is the low-mass, efficient power conditioning and a relatively effective acceleration mechanism.

2.5 Summary of Microthruster System Performance

We have reviewed various pulsed microthruster technologies and found that Laser Ablation Microthrusters fill a special niche for missions that require nNs minimum impulse bits for precise pointing. Diode-based systems could perhaps compete on a system-level with the μ PPT if the total mass can be decreased while the propellant throughput is increased reliably. Pulsed diode-pumped lasers permit ablation of a larger variety of materials including metals or non-essential spacecraft parts. However, due to the reduced laser system efficiency, this concept does not compare well to other microthruster systems unless ultra-precise positioning or a widely distributed

Criteria	Unit	LA μ T	μ PPT	VAT
Min. I_{bit}	μ Ns	0.001	2-10	\sim 1
Repeat., σ	\pm %	10-25	50-70	10-25
Max. Thrust	mN	0.1-0.25	0.1-1	0.5-2
I_{bit}/E or C_m	μ Ns/J	50-200	5-15	2-20
T/P, Eq. (2)	μ N/W	0.2-50	4-12	2-18
η_{pc} , Eq. (3)	%	0.1-25	\sim 80	\sim 90
η_{pu} , Eq. (5)	%	\sim 80	60-100	\sim 80
Dry Mass	kg	0.4-1	0.5-1	0.1-0.3
I_{sptot} , Eq. (1)	km/s	0.3-3	0.5-2	0.5-5
η_{sys} , Eq. (4)	%	0.01-1	\sim 1	0.5-5

Table 1: Comparison of various pulsed microthruster technologies. Values, where given, should be considered in broad terms as these devices are currently under rapid development. Data was taken from peer reviewed publications when possible, see Refs. [8, 11, 20, 21, 23, 24].

propulsion system is required.

3 Laser Ablation Experiment

To investigate propellant, performance, and lifetime issues as well as simply to familiarize ourselves with the technology, we have constructed a laser ablation experiment in an ultra-high vacuum (UHV) chamber. For this experiment, we chose two VEM 1064 T0-3 Synoptics Microlasers operating at 1064 and 532 nm with all-solid-state construction. The Synoptics Microlasers are diode pumped, passively Q-switched, Nd:YAG lasers that provide high intensity, nanosecond pulses capable of ablating a variety of materials. Furthermore, the low-mass, small size, ease of operation, commercial availability, and low cost also influenced our choice. A full list of specifications is given in Table (2) for the 532 nm laser which was used for all the studies presented here. This is a similar type of laser used by the group at Lincoln Laboratory, although slightly less energy per pulse. Still, with the proper optical setup, the fluence threshold for efficient ablation presented by Phipps, et al (see Section 2.2) can be met.

The purpose of these first experiments was three fold, 1) characterize the effects of background pressure, 2) observe the effects of using a fixed-location for ablation over a large number of pulses, and 3) determine the impact of changing pulse and burst rates. These questions originated from previous experimental observations of changes in performance of pulsed plasma thrusters due to different vacuum environments and variable pulse rates. Before

Parameter	Value
Wavelength	532 nm
Peak Output Power	5.6 kW
Pulse Energy	5 μ J
Max. SS Output Power	21 mW at 4.1 kHz
Pulsewidth (FWHM)	900 ps
Max. Pulse Frequency	4.1 kHz at 1.5 A
Laser Diode Current	1.4-1.5 A
Input Laser Power	2.7 W at 1.5 A
Active Cooling Power	3.5 W at 1.5 A
Total Laser Efficiency	0.3%
Mass of Laser Head	30.4 g

Table 2: Operating characteristics of Synoptics VEM 1064 T0-3 Microlaser. The entire microlaser fits in a T0-3 can.

performance can be characterized accurately, a method or procedure that addresses these concerns must be created. In addition, this information should be useful for designing and testing LA μ Ts in the future.

The experiment setup is shown in Figs. 1 and 2. This remainder of this section covers results including all the topics mentioned above. We also discuss the implications of these results for future tests of LA μ Ts.

3.1 Results

Multiple test cases were repeated using different pulse rates, burst rates, and different background pressures to characterize the peak ion velocity and current distribution over a variety of conditions. Peak ion velocity is determined by measuring the time-of-flight between the photodiode signal and the arrival of a the first sign of current collected at the Faraday probe 6 in. away. We will now discuss the results of three different experiments to determine the influences of background pressure, multiple pulses in the same location, and variable pulse and burst rates.

3.1.1 Effects of Background Pressure

Previous experience with pulsed plasma thrusters has shown that mono-layers of background gasses on electrodes can significantly influence performance [25]. As a rule of thumb, a mono-layer of background gases can be adsorbed on a surface in 1 s at 10^{-6} Torr, and proportionally faster at higher pressures. For that reason, we wanted to perform the majority of our testing at as low of

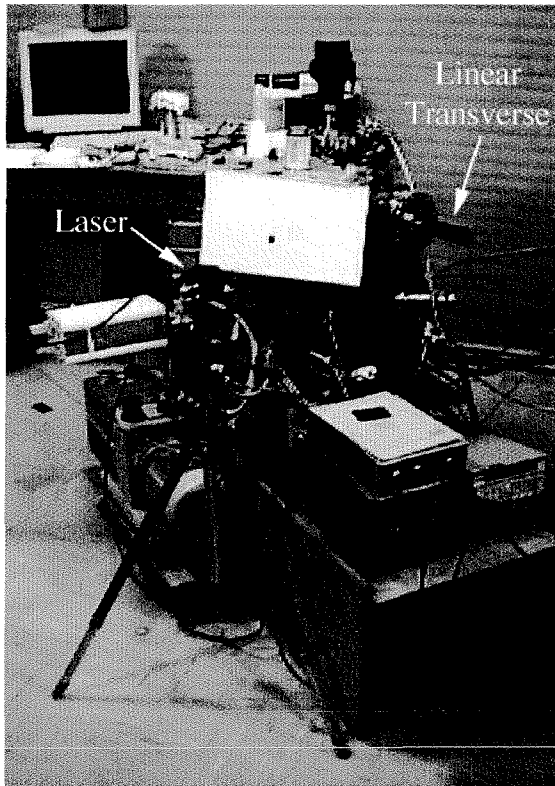


Figure 1: Picture of ultra-high vacuum chamber used for laser ablation experiments.

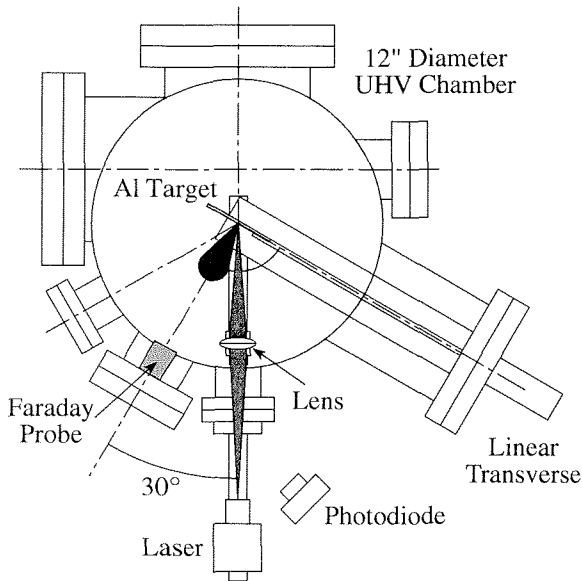


Figure 2: Drawing of the ultra-high vacuum chamber used for laser ablation experiment showing orientation of the laser, aluminum target, and linear feed-through.

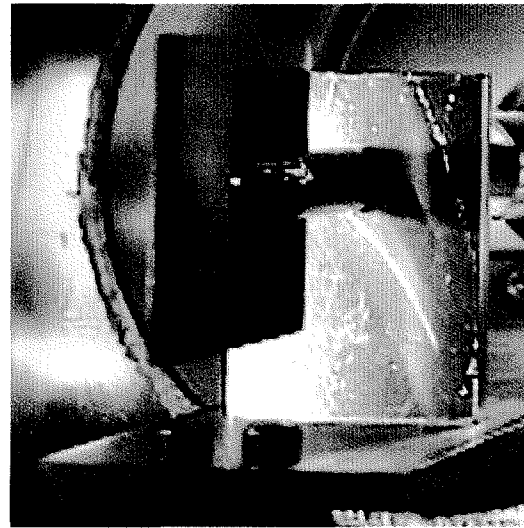


Figure 3: Close up photograph of the laser ablation experiment during operation. The aluminum target and sample holding arm are visible through a large window in the side of the chamber.

a pressure as possible, 10^{-7} Torr.

The results from this experiment are shown in Fig. (4). Note that the time of arrival of the first ions is similar in all the cases, except, perhaps for a slight decrease at 10^{-4} Torr. However, the current distribution is very different for each case. First, it should be noted that the limited frequency response of the current amplifier likely distorted these traces. Still, it is clear from the graph that the current density decreased with increasing pressure until the 10^{-4} Torr case. We suggest that at higher pressures mono-layers of background gases influence the measurements. Another possibility is simply that the ablation process itself has somehow changed. Although, as mentioned perviously, researchers have found differences in behavior at various pressure levels, usually it is a much more drastic change, from atmosphere to vacuum conditions, for example, that causes the change. In any case, it is clear from these results that background pressure should always be taken into account (or at least mentioned) in performance measurements, and performances measured in ground testing may be different from those produced in the hard vacuum of space. More tests at even lower pressures should be conducted to determine if an asymptote in current density exists below a given pressure.

3.1.2 Effects of Multiple Pulses

Although propellant feed systems can be designed to expose a fresh surface for each pulse, we wanted to examine

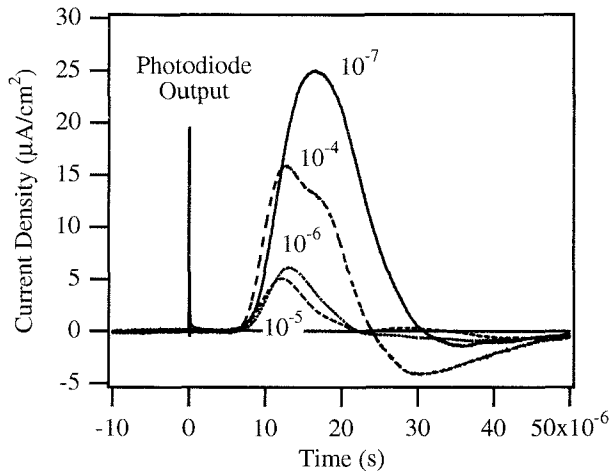


Figure 4: Effects of background pressure on current density measurements for single pulses on a fresh surface. Frequency response limits of the current amplifier may influence the curve shapes.

the effects of using a single site for ablation over multiple pulses. In addition, we used a 30° incident angle on the surface to examine the effects of off-normal ablation. Using some type of incident angle to protect optics has been suggested by both LA μ T research groups.

Figures 5 and 6 show graphs of peak ion velocity and current density as function of the pulse number. To investigate the effects of pulse timing, we also used three different values of the number of pulses per burst. The pulse frequency within a burst is close to 2 kHz while the time between bursts is close to 20 s (required time to download oscilloscope). There are two important trends that can be seen in the data.

First, the decay rate is smaller for 1 pulse/burst compared to either 5 pulses/burst or 10 pulses/burst until close to 200 pulses have been accumulated. We will discuss this trend in more detail in the next subsection. Second, the decay rate in the first few pulses is large, as much as 50%, and slows between about 5 and 50 pulses to almost no decay, or even a slight increase. At approximately 100 pulses there is another steep decline in ion velocity and current density. We believe this is a result of the incident angle of the laser. As shown in Fig. (9), a cone of target material begins to form in the direction of the laser after 100 pulses. As seen in the other images with fewer accumulated pulses, molten ejecta are clearly present. When the ablation site begins to penetrate into the target, steep walls and finally a cone of material is built up above the original surface. This cone could easily be directing the

exhaust plasma back towards the laser focusing optic and away from the Faraday probe. More experiments with a series of Faraday probes at various angles should be conducted to measure the evolution of the angular current distribution with pulse number.

3.1.3 Effects of Pulse Rate and Burst Rate

As mentioned in the previous sub-section, tests with different numbers of pulses/burst showed different rates of decay. To investigate this trend more carefully, we repeated the tests on each of the first 20 pulses in a series. For the 1 pulse/burst case, this consisted of 20 trials, each with approximately 20 seconds of delay from the previous trial. For the 5 pulses/burst case, only four trials were performed, and similarly for the 10 pulses/burst case, only two trials were necessary.

The results of these tests can be seen in Fig. (7) and Fig. (8). Note that the asymptote level in each case matches with what was measured in the previous experiment. In addition, for the 5 and 10 pulses per burst cases, the decay rate appears to be similar for the first five pulses in each burst. Again, in both cases nearly the same asymptote is reached just a few pulses. However, between each burst (or each pulse in the 1 pulse/burst case) the performance recovers to nearly the same level. Although the ion velocity and current density do not recover completely, the change is significant, nearly 60% in some cases. This indicates that either 1) the surface or target conditions are changing with time constants on the order of 10 seconds, or 2) the laser intensity increases on the first pulse in each burst after approximately 20 s of down-time. It should be noted that to modulate the laser, the diode-pump current is normally kept just below the lasing threshold and increased only slightly (0.12 A out of 1.4 A) to activate the laser. More tests using a residual gas analyzer and a more sensitive photodiode to detect laser power should be conducted to find the cause of these trends. In any case, whether the laser or target conditions are to blame, test results should be presented in the context of how many pulses have been accumulated on a fixed ablation site.

4 Conclusions

We have reviewed various pulsed microthruster technologies and found that Laser Ablation Microthrusters fill a special niche for missions that require nNs minimum impulse bits for precise pointing. Experimental measurements of peak ion velocity and current density were taken as a function of pulse number, pulse rate, burst rate, and background pressure. Each parameter was found to change the measurements with the most significant re-

sults that 1) background pressure changes between 10^{-4} and 10^{-7} Torr effect the performance, 2) normal-to-target ion velocity and current significantly decays after the first pulse at the same ablation site, 3) decay rates depend both on pulse and burst frequency, and 4) after approximately 100 pulses a cone of ejected material begins to block ion current in the direction normal to the target. From SEM images, it appears as if a cone pointing back towards the focusing optic is protruding from the surface after 100 pulses. These results could play an important role in future experimental and LA μ T designs.

Acknowledgements

The author wishes to acknowledge Jay Polk, Lee Johnson, and David Conroy of the Advanced Propulsion Technology Group at JPL for their significant contributions and insights. This work is funded under the Advanced Propulsion Concepts Program.

The research described in this paper was carried out at the Jet Propulsion Laboratory, California Institute of Technology, under a contract with the National Aeronautics and Space Administration.

References

- [1] J. Mueller. *Thruster Options for Microspacecraft: A Review and Evaluation of State-of-the-Art and Emerging Technologies*, volume 187 of *AIAA Progress in Astronautics and Aeronautics*, chapter 3. AIAA, 2000.
- [2] C.R. Phipps, J. Luke, and G.G. McDuff. A Diode-Laser-Driven Microthruster. In *27th International Electric Propulsion Conference*, Pasadena, California, October 15-19 2001. IEPC 01-220.
- [3] J. Luke, C.R. Phipps, and G.G. McDuff. Diode Laser Driven Microthruster Prototype. In *27th International Electric Propulsion Conference*, Pasadena, California, October 15-19 2001. IEPC 01-223.
- [4] C.R. Phipps, J. Luke, and J. Marquis. Diode Laser-based Microthrusters: A New Departure in High I_{sp} , Long-Life Engines. In *36th Joint Propulsion Conference*, Huntsville, Alabama, July 16-19 2000. AIAA 2000-3477.
- [5] C.R. Phipps, J. Luke, and G. McDuff. Laser Ablation Powered Mini-thruster. In *Proceedings of 2002 SPIE High-Power Laser Ablation Conference*, volume 4760, Taos, New Mexico, April 22-26 2002. SPIE 4760-104.
- [6] J. Luke, C.R. Phipps, and G. McDuff. Laser Plasma Thruster Continuous Thrust Experiment. In *Proceedings of 2002 SPIE High-Power Laser Ablation Conference*, volume 4760, Taos, New Mexico, April 22-26 2002. SPIE 4760-105.
- [7] D.A. Gonzales and R.P. Baker. Microchip Laser Propulsion for Small Satellites. In *37th Joint Propulsion Conference*, Salt Lake City, Utah, July 8-11 2001. AIAA 2001-3789.
- [8] D.A. Gonzales and R.P. Baker. Micropropulsion using a Nd:YAG Microchip Laser. In *Proceedings of 2002 SPIE High-Power Laser Ablation Conference*, volume 4760, Taos, New Mexico, April 22-26 2002. SPIE 4760-98.
- [9] I.D. Boyd and M. Keidar. Simulation of the Plume Generated by a Micro Laser-ablation Plasma Thruster. In *Proceedings of 2002 SPIE High-Power Laser Ablation Conference*, volume 4760, Taos, New Mexico, April 22-26 2002. SPIE 4760-106.
- [10] A.V. Pakhomov and D.A. Gregory. Ablative Laser Propulsion: An Old Concept Revisited. *AIAA Journal*, 38(4):725–727, 2000.
- [11] C.R. Phipps and J. Luke. Diode Laser-Driven Microthrusters: A New Departure for Micropropulsion. *AIAA Journal*, 40(2):310–318, 2002.
- [12] C.R. Phipps et al. Impulse Coupling to Targets in Vacuum by KrF, HF, and CO₂ Lasers. *JOURNAL OF APPLIED PHYSICS*, 64(3):1083–1096, 1988.
- [13] F. Dahmani. Experimental Scaling Laws for Mass-Ablation Rate, Ablation Pressure in Planar Laser-Produced Plasmas with Laser Intensity, Laser Wavelength, and Target Atomic-Number. *JOURNAL OF APPLIED PHYSICS*, 74(1):622–634, 1993.
- [14] P. Hammerling and J.L. Remo. Ablation Scaling Laws for Laser Space Debris Clearing. In *Proceedings of 1998 SPIE High-Power Laser Ablation Conference*, volume 3343, Sante Fe, New Mexico, April 1998.
- [15] A.G. Guidoni, R. Kelly, A. Mele, and A. Miotello. Heating effects and gas-dynamic expansion of the plasma plume produced by irradiating a solid with laser pulses. *PLASMA SOURCES SCIENCE & TECHNOLOGY*, 6(3):260–269, 1997.
- [16] R.E. Russo, X.L. Mao, H.C. Liu, J.H. Yoo, and S.S. Mao. Time-resolved plasma diagnostics and mass removal during single-pulse laser ablation.

APPLIED PHYSICS A-MATERIALS SCIENCE & PROCESSING, 69(S):S887–S894, 1999.

- [17] R. Kelly. On The Dual Role of The Knudsen Layer And Unsteady, Adiabatic Expansion In Pulse Sputtering Phenomena. *JOURNAL OF CHEMICAL PHYSICS*, 92(8):5047–5056, 1990.
- [18] A.V. Gusarov, A.G. Gnedovets, and I. Smurov. Gas dynamics of laser ablation: Influence of ambient atmosphere. *JOURNAL OF APPLIED PHYSICS*, 88(7):4352–4364, 2000.
- [19] J.J. Zayhowski. Passively Q-switched Nd : YAG microchip lasers and applications. *JOURNAL OF ALLOYS AND COMPOUNDS*, 303:393–400, 2000.
- [20] F.S. Gulczinski, M.J. Dulligan, J.P. Lake, and G.G. Spanjers. Micropropulsion Research at AFRL. In *36th Joint Propulsion Conference*, Huntsville, Alabama, July 16-19 2000. AIAA 2000-3255.
- [21] R.A. Spores, G.G. Spanjers, M. Birkan, and T.J. Lawrence. Overview of the USAF Electric Propulsion Program. In *37th Joint Propulsion Conference*, Salt Lake City, Utah, July 8-11 2001. AIAA 2001-3225.
- [22] M. Martin. Distributed Satellite Missions and Technologies - The TechSat 21 Program. In *AIAA Space Technology Conference & Exposition*, Albuquerque, NM, September 28-30 1999. AIAA 99-4479.
- [23] J. Schein, N. Qi, R. Binder, M. Krishnan, J.K. Ziemer, J.E. Polk, and A. Anders. Low Mass Vacuum Arc Thruster System for Station Keeping Missions. In *27th International Electric Propulsion Conference*, Pasadena, California, October 15-19 2001. IEPC 01-238.
- [24] J. Schein, N. Qi, R. Binder, M. Krishnan, J.K. Ziemer, J.E. Polk, and A. Anders. Inductive Energy Storage Driven Vacuum Arc Thruster. *Review of Scientific Instruments*, 73(2):925–927, 2002.
- [25] J.K. Ziemer, E.Y. Choueiri, and D. Birx. Is the Gas-Fed PPT an Electromagnetic Accelerator? An Investigation Using Measured Performance. In *35th Joint Propulsion Conference*, Los Angeles, California, June 20-24 1999. AIAA 99-2289.

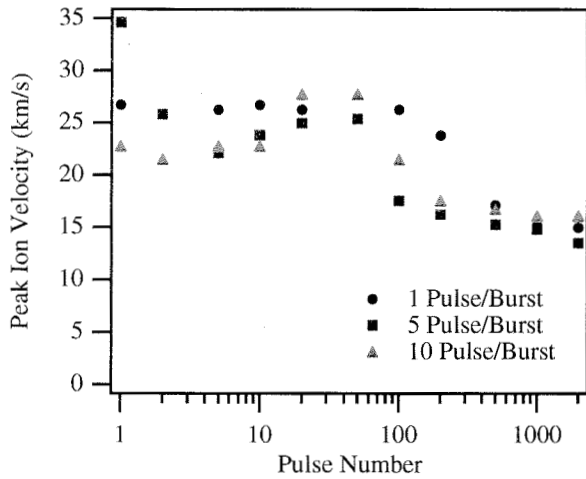


Figure 5: Graph of peak ion velocity based on time of flight data from Faraday probe over 2000 pulses. Time between bursts is 20 sec and time between pulses within a burst is 0.5 ms. Error is $\pm 10\%$ due to frequency response limits of the current amplifier.

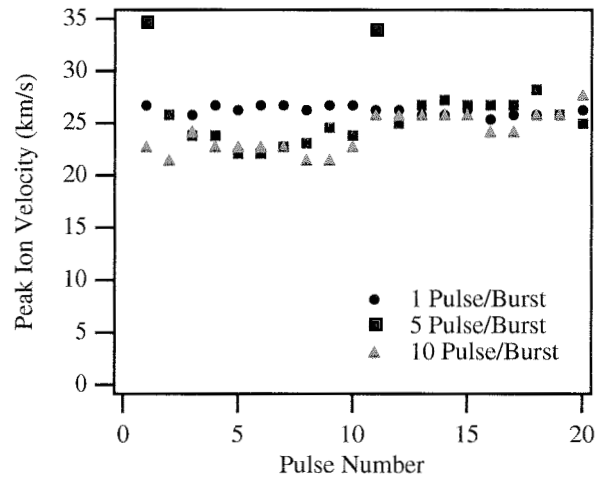


Figure 7: Graph of peak ion velocity based on time of flight data from Faraday probe over the first 20 pulses. Time between bursts is 20 sec and time between pulses within a burst is 0.5 ms. Error is $\pm 10\%$ due to frequency response limits of the current amplifier.

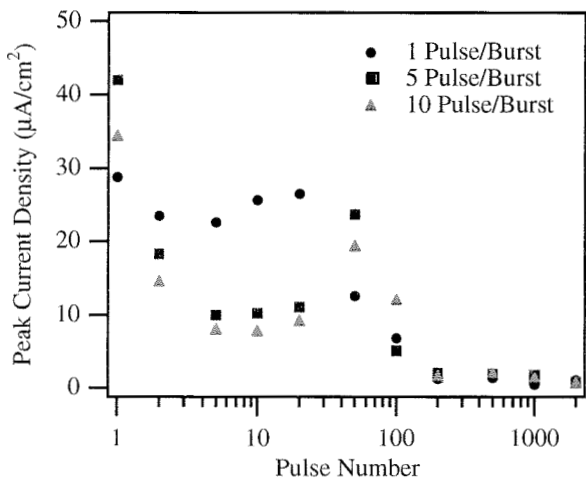


Figure 6: Graph of peak current density collected at the faraday probe normal to the target over 2000 pulses. Time between bursts is 20 sec and time between pulses within a burst is 0.5 ms.

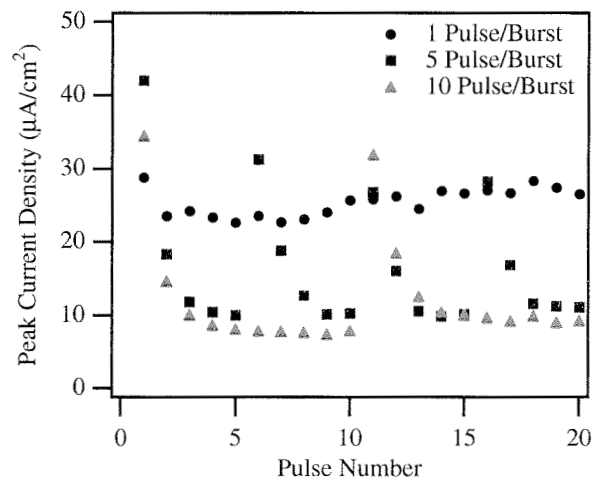


Figure 8: Graph of peak current density collected at the faraday probe normal to the target over 2000 pulses. Time between bursts is 20 sec and time between pulses within a burst is 0.5 ms.

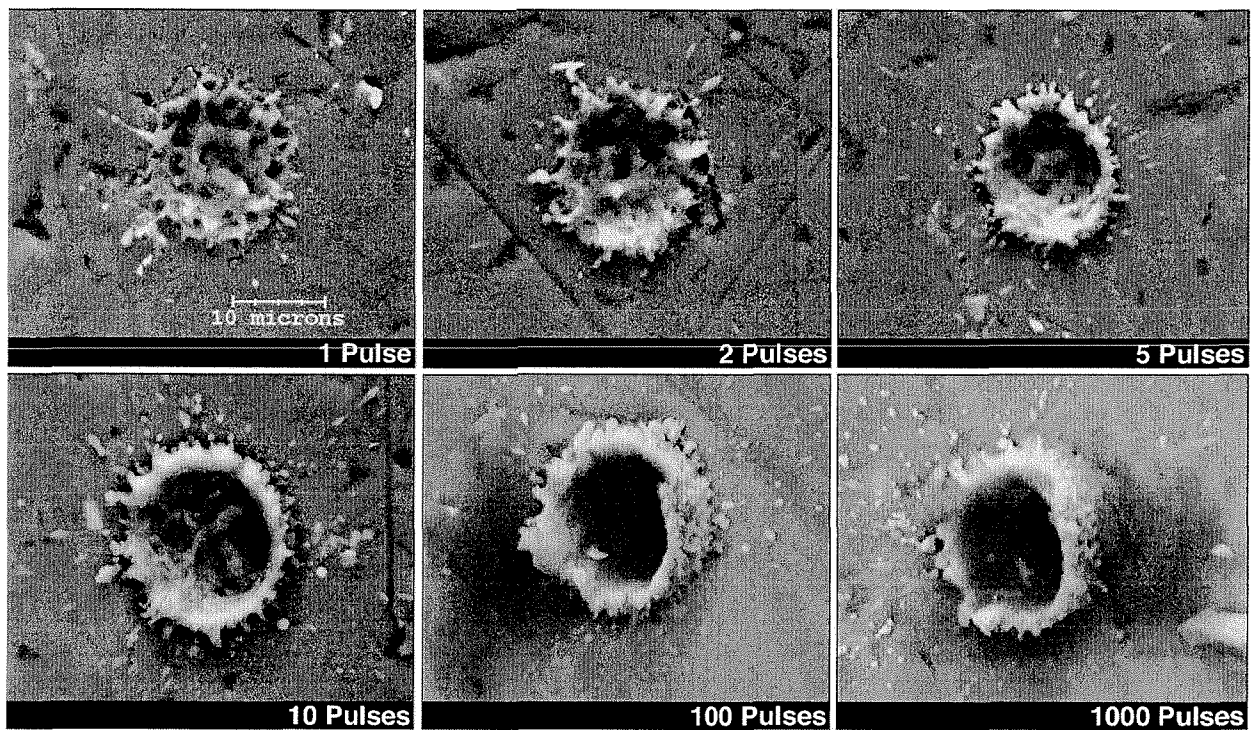


Figure 9: Electron micrograph images of multiple pulse ablation sites on an aluminum target. Each ablation process started with a fresh surface. A ten micron sized scale is shown in the upper left image, and each image is magnified by the same amount. The laser source comes from 30° to the left of normal as viewed in these images.